### INTERNATIONAL JOURNAL OF OPTIMIZATION IN CIVIL ENGINEERING Int. J. Optim. Civil Eng., 2025; 15(3):389-417



### SEISMIC PERFORMANCE-BASED TOPOLOGY OPTIMIZATION AND COLLAPSE ANALYSIS OF STEEL SHEAR WALL SYSTEMS

K. Farzad\*,† and S. Ghaffari
Faculty of Engineering, Islamic Azad University, Urmia, Iran

#### **ABSTRACT**

The use of steel shear wall systems has increased significantly in recent years as an effective solution for resisting lateral loads in buildings. This study focuses on the seismic collapse safety assessment of steel frames with optimal positions of steel shear walls obtained through various metaheuristic optimization algorithms and concepts of performance-based design methodology. Due to potential irregularities and discontinuities in the lateral load-resisting system and the limitations of code-based linear analysis, nonlinear pushover analyses with multiple lateral load patterns are employed to estimate key structural responses during the optimization process. The seismic collapse performance of the optimized frames is further evaluated using the FEMA P-695 methodology, which involves nonlinear dynamic analysis to assess collapse capacity. The primary objective is to examine the influence of steel plate shear wall placement on the structural weight optimization of steel frames. To this end, two case studies, a 10-story and a 15-story steel frame equipped with steel shear walls, are presented. The results demonstrate the critical role of shear wall location in achieving optimal structural designs.

**Keywords:** Steel shear wall system, incremental dynamic analysis, performance-based design, metaheuristic algorithms, structural shape optimization.

Received: 27 July 2025; Accepted: 19 September 2025

#### 1. INTRODUCTION

In engineering design, a fundamental objective is to minimize project costs while simultaneously ensuring that the structure meets required performance criteria. Achieving

<sup>\*</sup>Corresponding author: Department of Civil Engineering, Urmia Azad University, Urmia, Iran

<sup>†</sup>E-mail address: keyvan.farzad@iau.ac.ir (K. Farzad)

this balance lies at the core of structural optimization, where efficiency, safety, and economy are integrated into the design process. In seismic regions, this objective becomes even more critical due to the complex and distinct behavior of structural systems under lateral and gravitational loads. As a result, developing structural systems that are both seismically resilient and cost-effective is essential for reliable and efficient performance during earthquake events.

As structural optimization problems become increasingly complex, traditional analytical and deterministic methods often prove inadequate or inefficient. In response, metaheuristic algorithms have emerged as powerful alternative tools for solving high-dimensional, nonlinear, and multi-objective optimization problems. These algorithms—many of which are inspired by natural or biological processes—are capable of escaping local optima and converging toward global solutions without requiring gradient information or differentiability. In structural engineering, such metaheuristic approaches have been widely adopted and further developed to enhance design efficiency and reduce construction costs, particularly in the context of large-scale and performance-sensitive systems.

With the increasing complexity of structural systems and the inherently unpredictable nature of earthquakes, traditional linear analysis methods have often resulted in overly conservative and uneconomical designs. To address these limitations, the performance-based design (PBD) approach has been developed and widely adopted. This methodology emphasizes nonlinear analysis to more accurately assess a structure's ability to achieve predefined performance objectives under varying levels of seismic intensity. The overarching goals of performance-based design include safeguarding human life, minimizing economic and environmental losses, and aligning structural performance with the specific objectives and risk tolerance of stakeholders, particularly under critical loading scenarios[1,2].

In steel structure design, bracing systems are widely recognized as one of the most effective methods for resisting lateral loads. A key challenge in their design lies in determining the optimal configuration of member sections and the precise placement of the lateral bracing system. Traditionally, these decisions have often been based on the designer's experience and judgment. However, such heuristic approaches may not yield globally optimal solutions, especially given the nonlinear and complex behavior of large structural systems. Even minor modifications in member cross-sections or bracing locations can significantly influence the overall structural response. Therefore, the application of systematic optimization techniques offers a powerful means to improve design efficiency and structural performance in this context [3].

The performance-based seismic design (PBSD) approach is grounded in the principle that a structure must satisfy defined performance objectives and maintain acceptable safety levels under earthquakes of varying intensity and return periods. This approach enables designers to explicitly consider the expected seismic performance of a structure across different hazard levels. Optimization techniques can be effectively integrated into the PBSD framework, where structural performance metrics—such as interstory drift, ductility demand, or collapse capacity—are treated as objective functions or constraints. This integration allows for the development of design solutions that are not only performance-compliant but also structurally and economically efficient [4,5].

The primary objective of this research is to determine the optimal placement of steel plate

shear walls (SPSWs) within steel frame structures using advanced metaheuristic optimization algorithms. Over the past two decades, SPSWs have emerged as a viable alternative to traditional lateral load-resisting systems such as reinforced concrete shear walls and braced frames. This structural system offers several notable advantages, including high ductility, substantial initial stiffness, ease of construction, and a reduction in overall structural mass. These characteristics make SPSWs particularly suitable for seismic applications where both strength and deformation capacity are critical[6].

Moreover, experimental studies have demonstrated that the post-buckling behavior of steel plate shear walls, characterized by stable and energy-dissipating hysteretic response, is often more effective in seismic performance than purely elastic behavior[7].

In recent years, metaheuristic algorithms have gained significant popularity in solving complex engineering problems due to their high efficiency, adaptability, and relatively low computational cost. Unlike traditional optimization methods, metaheuristic algorithms are not restricted to specific problem types and can be applied across a wide range of applications. Each algorithm employs a unique formulation and search strategy to explore the solution space and converge toward a global optimum. In this study, three widely used metaheuristic algorithms - the modified Dolphin algorithm [8], the center of mass algorithm [3], and the Gray Wolf (GWO) algorithm [9] - are used to optimize the sections and placement of steel shear walls in steel frames. These algorithms have demonstrated strong performance in prior research, particularly in problems involving structural systems similar to those considered in this work.

Optimal design of structures subjected to seismic loads remains a challenging and complex problem in structural engineering. While nonlinear time history analysis offers the most accurate assessment of seismic response, its high computational demand often limits its use within optimization procedures. Consequently, simpler methods such as nonlinear static (pushover) analysis or linear dynamic analysis are typically employed during the optimization phase, with final designs validated through more rigorous dynamic analyses. In this study, Incremental Dynamic Analysis (IDA) is utilized to comprehensively evaluate the seismic performance of the optimized structures. IDA provides detailed insight by systematically subjecting the structure to a suite of scaled ground motion records, enabling the assessment of structural response over a wide range of seismic intensities [10,11].

In this study, 10- and 15-story two-dimensional steel frame structures equipped with steel shear wall systems are optimized using performance-based design principles. Nonlinear pushover analyses with various lateral load patterns are employed within the optimization process, utilizing multiple metaheuristic algorithms. Subsequently, the seismic collapse safety of the optimized frames is evaluated through Incremental Dynamic Analysis (IDA). Numerical results highlight the significant influence of shear wall placement along the building height on structural performance and demonstrate that the optimized frames achieve acceptable seismic collapse safety levels.

## 2. PERFORMANCE-BASED DESIGN OF STEEL PLATE SHEAR WALL SYSTEM

Performance-based design involves three main steps:

#### A) Definition of Performance Objectives

The first step involves defining performance objectives, which are combinations of seismic hazard levels and corresponding structural performance expectations. Hazard levels range from low-intensity earthquakes with short return periods to high-intensity events with long return periods. Structural performance can be evaluated based on criteria such as physical damage or economic loss. In this study, following the guidelines of FEMA 356[12] and ASCE/SEI 41-17[13], three performance levels are defined: Immediate Occupancy (Uninterrupted Serviceability), Life Safety, and Collapse Prevention. These levels represent increasing degrees of structural demand and are used to evaluate the acceptability of the structural response under different seismic scenarios.

To accurately define performance objectives within a performance-based design framework, it is essential to consider multiple seismic hazard levels. Typically, three primary hazard levels are employed:

- Hazard Level 1 Operational-Level Earthquake (OLE): Represents a frequent, low-intensity event with a 50% probability of exceedance in 50 years (approximately 72-year return period).
- Hazard Level 2 Design Basis Earthquake (DBE): Corresponds to a moderate seismic event with a 10% probability of exceedance in 50 years (475-year return period).
- Hazard Level 3 Maximum Considered Earthquake (MCE): Represents a rare, high-intensity event with a 2% probability of exceedance in 50 years (2,475-year return period).

These hazard levels are used to correlate expected ground motions with targeted structural performance levels, thereby enabling a more rational and risk-informed design approach.

# B) Determining the seismic capacity of the structure and its components through mathematical model analysis

Following the definition of performance objectives and the assessment of structural capacity, the next step involves evaluating whether the design meets the specified performance criteria. In this study, nonlinear static (pushover) analysis is employed to estimate the structural capacity and assess compliance with performance targets. Initially, the structure must demonstrate adequate performance under gravity loads and service-level conditions, in accordance with AISC-LRFD provisions [14]. Once these basic requirements are met, the structure is evaluated at each defined performance level through nonlinear analysis.

To simulate realistic load conditions during pushover analysis, gravity loads acting on the beams are determined based on the load combination Q = 1.1(DL + 0.25 LL) as recommended by FEMA 356. The target displacement for the analysis is also calculated in accordance with FEMA 356, using Equation 1,

$$\delta_t = C_0 C_1 C_2 C_3 S_a \frac{T_e^2}{4 \pi^2} g \tag{1}$$

In this equation,  $T_e$  represents the effective fundamental period of the structure in the direction of analysis, and  $S_a$  is the spectral acceleration corresponding to  $T_e$ , determined for

each performance level. In this study,  $S_a$  values are obtained based on a Soil Type D site classification, following the spectral response curves provided in Figure 1[15]. All additional coefficients and parameters required for the calculation are adopted as specified in the FEMA 356 guidelines.

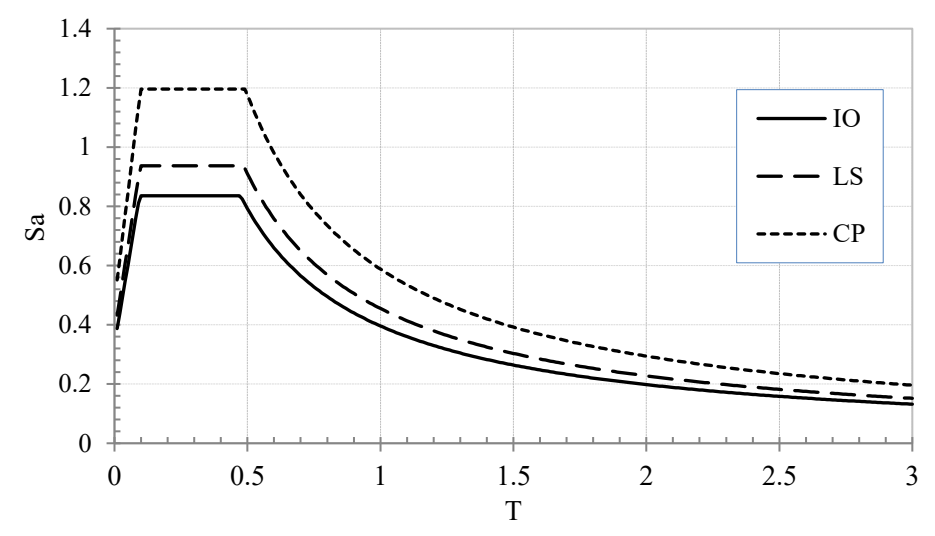


Figure 1: Response spectrum curve

The lateral force distribution pattern in the height of the building is according to formula 2:

$$C_{vx} = \frac{W_x h_x^k}{\sum_{i=1}^n W_i h_i^k} \tag{2}$$

 $C_{vx} = \frac{w_x h_x^k}{\sum_{i=1}^n w_i h_i^k}$  (2) where  $w_i$  is the weight of the *i*th floor,  $h_i$  is the height of the *i*th floor, and k is calculated according to the following equation:

$$k = \begin{cases} 2 & for & T \ge 2,5 \text{ seconds} \\ 1 & for & T \le 0,5 \text{ seconds} \end{cases}$$
 (3)

For intermediate values of T, the value of k is calculated using interpolation.

FEMA 356 emphasizes that pushover analysis should be conducted using at least two different lateral load patterns to capture a range of structural responses. In this study, two lateral load patterns are employed: (1) a pattern based on the code coefficient  $C_{vx}$  (Formula 2), and (2) a uniform lateral load distribution proportional to the mass at each story level. To further account for the effects of higher vibration modes and improve the accuracy and practicality of the analysis, a modal pushover analysis approach is also utilized. This method combines the responses from multiple modes of vibration according to the modal combination procedure defined in Formula 4 [16].

$$F_j = \Sigma \alpha_n \Gamma_n m \bar{\phi}_n S_n(\xi_n, T_n) \tag{4}$$

where  $\alpha_n$  is the modal correction factor, which can take positive or negative values depending on the mode and structural characteristics;  $\phi_n$  is the mode shape vector corresponding to the nth vibration mode; and  $S_n$  represents the spectral acceleration associated with the natural period of the nth mode. This formulation allows the modal pushover analysis to effectively incorporate the influence of multiple vibration modes on the lateral load distribution and resulting structural response and:

$$\Gamma = \frac{[\phi]^T[m]\{l\}}{M_n} \text{ in which } M_n = [\phi]^T[m][\phi]$$
 (5)

The responses received will be the maximum values provided by the three lateral load patterns above.

## C) Evaluating Structural Performance and Verifying Compliance with Functional Objectives

In the analysis and design of steel shear wall frames, two primary objectives must be achieved. The first is to ensure that internal forces—such as axial and bending forces in boundary elements, as well as tensile forces in the steel plate—comply with code requirements, thereby controlling the sizing of these components. The second objective is to limit lateral displacements of the structural system to acceptable levels, ensuring that the overall seismic performance meets the prescribed criteria set forth by relevant design codes.

The design of steel shear walls, as detailed in Berman's studies [17], involves thin, unstiffened steel plates connected to horizontal boundary elements (HBEs or beams) and vertical boundary elements (VBEs or columns). Under in-plane lateral loading, the steel plate experiences shear buckling, resulting in the formation of diagonal tension fields that effectively resist lateral forces [18,19,20]. Figure 2 illustrates the detailed modeling approach of a steel shear wall system used in this study.

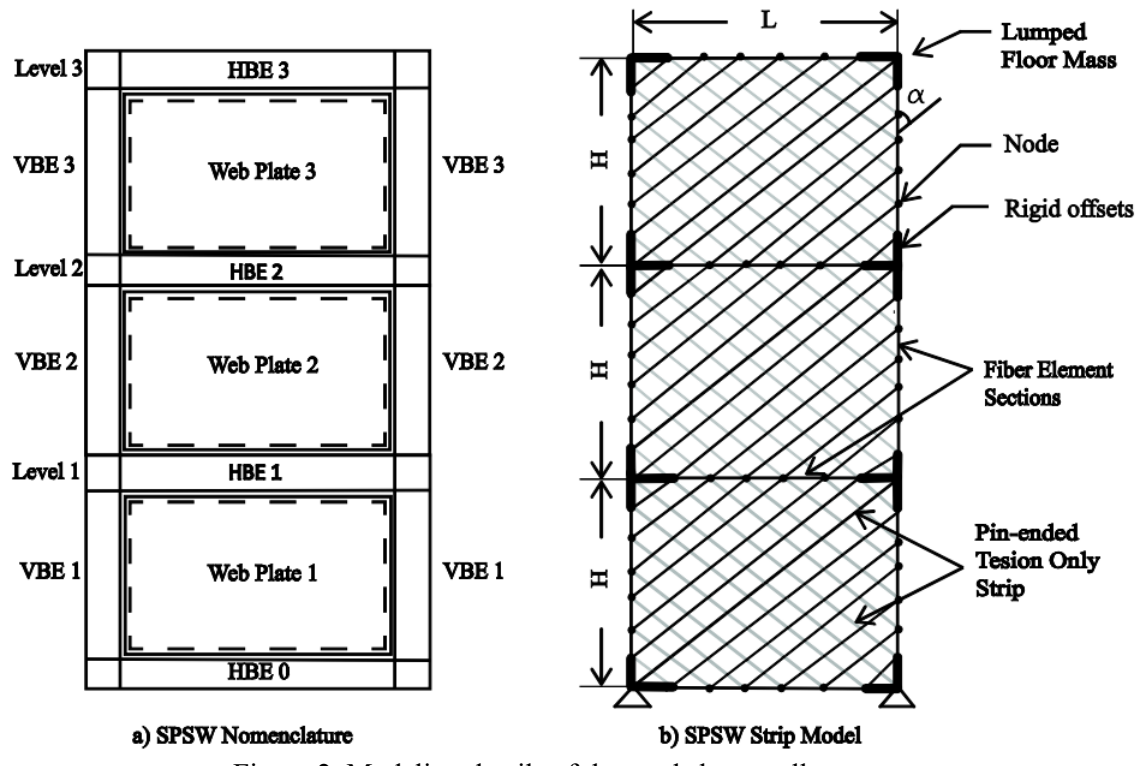


Figure 2. Modeling details of the steel shear wall system

In this study, the strip model approach is employed for finite element modeling of steel plate shear walls (SPSWs) within the OpenSees software framework. This method has demonstrated strong capability in accurately predicting both the ultimate capacity [19] and cyclic response [17] of shear walls. The strip modeling technique was selected primarily due to its computational efficiency, which is particularly advantageous given the large number of analyses required throughout the optimization process.

In the model, the steel plate elements are represented by linear truss elements with pinned (hinged) ends, which are configured to resist tension only. These elements utilize a hysteretic material model to capture the cyclic behavior of the steel, as illustrated in Figure 3.

The angle  $\alpha$ , which denotes the orientation of the tensile diagonal tension field formed in the steel plate after shear buckling, can be determined using Equation 6 [18,19].

$$tan^{4}\alpha = \frac{1 + \frac{t \cdot L}{2A_{c}}}{1 + t \cdot h\left(\frac{1}{A_{b}} + \frac{h^{3}}{360I_{c} \cdot L}\right)}$$
(6)

In this formula, t represents the thickness of the steel plate in the shear wall, L denotes the width of the shear wall, and h is the height of the wall. Additionally,  $A_b$  and  $A_c$  correspond to the cross-sectional areas of the horizontal boundary element (HBE) and vertical boundary element (VBE), respectively, while  $I_c$  represents the moment of inertia of the VBE. In the finite element model, all connections between VBEs and HBEs are assumed to be fully fixed (clamped) to accurately simulate the boundary conditions.

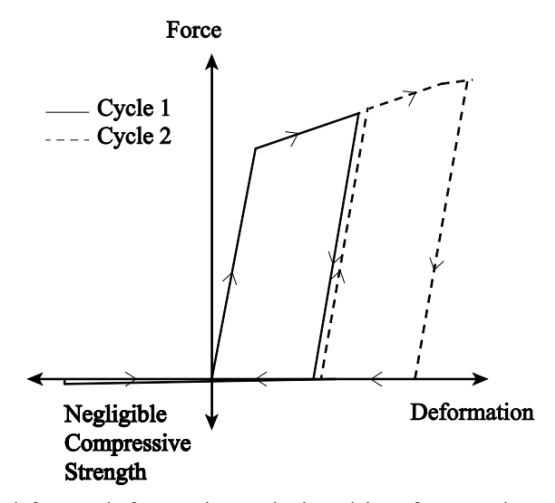


Figure 3. Axial force-deformation relationship of truss element in strip model

The horizontal boundary elements (HBEs) and vertical boundary elements (VBEs) are modeled as nonlinear beam-column elements with distributed plasticity, utilizing fiber-based cross-sectional definitions. To capture second-order effects, P-Delta phenomena are incorporated for all elements through the use of corotational geometric transformation commands in the mathematical model.

#### 3. METAHEURISTIC ALGORITHMS

Metaheuristic algorithms have been extensively applied to engineering problems due to their high flexibility, global search capability, and relatively low computational cost. Unlike traditional optimization methods, these algorithms are not restricted to specific problem types and can be effectively employed across a wide range of complex, nonlinear, and high-dimensional optimization tasks. Each metaheuristic algorithm employs a unique search strategy and formulation to explore the solution space and converge toward a global optimum. In this study, three widely used metaheuristic algorithms—previously validated in similar structural optimization research—are employed to optimize the configuration and design of steel frame structures with shear wall systems.

In this study, three metaheuristic algorithms—described in detail in this section—are utilized to optimize both the layout (shear wall placement) and the cross-sectional properties of steel frame structures equipped with steel shear wall lateral load-resisting systems. Based on their respective formulations, these algorithms have demonstrated the capability to effectively address the types of complex optimization problems investigated in this research[8,3,21].

#### 3.1 Modified Dolphin echolocation Algorithm (MDE)

Many human-developed technologies are inspired by natural processes. Dolphins, regarded as one of the most intelligent species after humans, use acoustic localization as a form of biological sonar to detect and track prey. Drawing inspiration from this behavior, the Dolphin Echolocation Algorithm simulates the search process within a design space, mimicking the way dolphins use echolocation to explore and identify optimal hunting paths[22].

The main steps of MDE are as follows:

- 1. Set random location coordinates for the dolphin.
- 2. Using Eq.7, the predefined probability (PP) assigned to the responses was determined.

$$PP(L_i) = PP_1 + (1 - PP_1) \frac{L_i^{Power}}{(LoopsNumber)^{power} - 1}$$
(7)

where  $PP(L_i)$  is a predefined probability in step i,  $PP_1$  is predetermined probability in step one,  $L_i$  is the current step number, and LoopsNumber is the number of steps in which the algorithm must achieve the optimal solution.

- 3. Calculate the fitness of each dolphin.
- 4. The fitness of each location is distributed to its neighbors using a symmetric triangular distribution or another symmetric distribution.
- 5. All devoted fitness values are added to each variable at every location to compute the accumulative fitness (AF). The cumulative fitness for variable j at position i is obtained using the following equation:

$$AF_{(A+k)j} = \frac{1}{R_e} (R_e - |K|) * Fitness(i) + AF_{(A+k)j}$$
 (8)

 $R_e$  is the effective radius.

where  $AF_{(A+k)j}$  is cumulative fitting, and A refers to the option chosen for the variable j located in i position. The value of k also varies from  $-R_e$  to  $R_e$ .  $R_e$  is defined as an effective radius within which the cumulative fitness around A is influenced by its own fitness. In the modified dolphin echolocation algorithm,  $R_e$  is set to one-quarter of the search range for the corresponding variable.

6. A small value  $\varepsilon$  is added to the accumulative fitness (AF) matrix to prevent premature convergence to local optima. The choice of  $\varepsilon$  depends on the definition of fitness and is preferably less than or equal to the minimum possible fitness value.

$$\varepsilon = AF + \varepsilon \tag{9}$$

- 7. Find the best location achieved and set its AF to zero.
- 8. Calculate the probability by normalizing AF as:

$$P_{ij} = \frac{AF_{ij}}{\sum_{i=1}^{LAj} AF_{ij}}$$
 (10)

where  $P_{ij}$  is the probability of the *i*th alternative to appear in the *j*th dimension.  $AF_{ij}$  is the accumulative fitness of the *i*th alternative to be in the *j*th dimension.

- 9. Select  $PP(L_i)$  percent of next step locations from best location dimensions. Distribute other values according to  $P_{ij}$ .
- 10. Repeat steps 2–9 for as many times as the Loops Number is.

#### 3.2 Center of mass optimization algorithm (CMO)

The Center of Mass Optimization (CMO) algorithm is inspired by the physical principle of the center of mass and is designed to solve complex optimization problems with high efficiency using only a single tuning parameter. In this algorithm, search agents are assigned mass values proportional to their fitness, and agents with greater mass exert a stronger influence on the system, attracting others toward the center of mass. Conversely, agents with lower mass are more influenced by the movement of others. This mass-based interaction forms the foundation of the search mechanism within the design space [3].

In the CMO algorithm, the mass of each search agent is calculated from the following equation:

$$m_i = \frac{1}{fit_i} \tag{11}$$

where  $fit_i$  is the fitness value of the objective function for the *i*th agent position.

In the CMO algorithm, search agents are classified into two groups based on their fitness: higher-quality agents (larger masses) and lower-quality agents (smaller masses). Each superior agent is then updated by considering its interaction with an inferior agent, specifically based on the distance between them. This mechanism promotes both exploration and exploitation of the design space by simulating gravitational-like attraction influenced by fitness-based mass differentiation.

For each pair of particles in the lth iteration and for each ith agent, the position of the center of mass ( $X^C$ ) and the inter-particle distance (Dl) are calculated using the following expressions:

$$X_{i}^{C}(l) = \frac{m_{i}X_{i}(l) + m_{\frac{nop}{2} + i}X_{\frac{nop}{2} + i}(l)}{m_{i} + m_{\frac{nop}{2} + i}}, \quad i = 1, 2, ..., \frac{nop}{2}$$

$$(12)$$

$$Dl_i(l) = \left| X_i(l) - X_{\frac{nop}{2} + i}(l) \right|, \quad i = 1, 2, ..., \frac{nop}{2}$$
 (13)

where nop represents the number of particles.

One of the most important characteristics of the CMO algorithm is its ability to maintain a balance between exploration and exploitation throughout the optimization process. Initially, the algorithm emphasizes exploration to broadly search the design space, while over successive iterations, the focus gradually shifts toward exploitation to refine the solution near optimal regions. In the CMO algorithm, particle positions are updated using the following formulation:

In the first step, a control parameter (CP) is introduced, which gradually decreases from 1 to 0 over the course of the optimization process.

$$CP(l) = exp\left(-\frac{5l}{l_{max}}\right) \tag{14}$$

where  $l_{max}$  is the maximum number of optimization iterations.

If the value of  $Dl_i$  exceeds the control parameter CP, the position of the *i*th particle pair is updated in the exploration phase according to the following equation:

$$X_{i}(l+1) = X_{i}(l) - r.\left(X_{i}^{C}(l) - X_{i}(l)\right) + r.\left(X_{best}(l) - X_{i}(l)\right)$$
(15)

$$X_{\frac{nop}{2}+i}(l+1) = X_{\frac{nop}{2}+i}(l) + r.\left(X_{i}^{C}(l) - X_{\frac{nop}{2}+i}(l)\right) + r.\left(X_{best}(l) - X_{\frac{nop}{2}+i}(l)\right)$$
(16)

If the value of  $Dl_i$  is less than the control parameter CP, the position of the *i*th particle pair is updated during the exploitation phase using the following expression:

$$X_{i}(l+1) = X_{i}(l) + r \cdot \left(X_{i}(l) - X_{\frac{nop}{2} + i}(l)\right)$$
(17)

$$X_{\frac{nop}{2}+i}(l+1) = X_{\frac{nop}{2}+i}(l) + r.\left(X_{i}(l) - X_{\frac{nop}{2}+i}(l)\right)$$
(18)

In the above expressions, r represents a uniformly distributed random number between 0 and 1, and  $X_{best}$  denotes the best solution identified up to the current iteration.

#### 3.3 Modified Gray Wolves Algorithm Using the K-Nearest Neighbor Algorithm(GWO-KNN)

The Grey Wolf Optimizer (GWO) algorithm is inspired by the social hierarchy and hunting behavior of grey wolves. In a typical wolf pack, the hierarchy is structured into four levels: alpha (the leader), beta (the advisor), delta (subordinate wolves), and omega (followers). In the GWO algorithm, the top three solutions found during the optimization process represent the alpha, beta, and delta wolves, while the remaining candidate solutions are considered omega. The optimization is carried out by mimicking the wolves' hunting strategy, which consists of three main phases: tracking (search), encircling the prey (exploitation), and attacking the prey (convergence) [21].

The encircling behavior of grey wolves during the hunting process is mathematically modeled by the following equation:

$$\vec{D} = \left| \vec{C}, \overrightarrow{X_p}(t) - \vec{X}(t) \right| \tag{19}$$

$$\vec{X}(t+1) = \vec{X}_p(t) - \vec{A}, \vec{D} \tag{20}$$

where t represents the current iteration, A and C are the coefficient vectors,  $X_p$  is the prey location vector, and X is the gray wolf location vector.

$$\vec{A} = 2\vec{\alpha}, \vec{r_1} - \vec{\alpha} \tag{21}$$

$$\vec{C} = 2\vec{r_2} \tag{22}$$

$$\vec{C} = 2\vec{r_2} \tag{22}$$

where the component  $\vec{\alpha}$  decreases linearly from 2 to 0 with increasing iterations of the algorithm. Also, the coefficients  $\vec{r_1}$  and  $\vec{r_2}$  are chosen randomly in the interval [0,1].

Gray wolves identify and surround prey with the guidance of alpha and the participation of beta and delta. In optimization, the top three positions (alpha, beta, delta) are considered the main solutions and the other solutions are updated according to them by the following formula.

$$\overrightarrow{D_{\alpha}} = |\overrightarrow{C_1}, \overrightarrow{X_{\alpha}} - \overrightarrow{X}|. \overrightarrow{D_{\beta}} = |\overrightarrow{C_2}, \overrightarrow{X_{\beta}} - \overrightarrow{X}|. \overrightarrow{D_{\delta}} = |\overrightarrow{C_3}, \overrightarrow{X_{\delta}} - \overrightarrow{X}|$$
(23)

$$\overrightarrow{X_1} = \overrightarrow{X_{\alpha}} - \overrightarrow{A_1}, (\overrightarrow{D_{\alpha}}).\overrightarrow{X_2} = \overrightarrow{X_{\beta}} - \overrightarrow{A_2}, (\overrightarrow{D_{\beta}}).\overrightarrow{X_3} = \overrightarrow{X_{\delta}} - \overrightarrow{A_3}, (\overrightarrow{D_{\delta}})$$
 (24)

$$\overrightarrow{X}_{1} = \overrightarrow{X}_{\alpha} - \overrightarrow{A}_{1}, (\overrightarrow{D}_{\alpha}).\overrightarrow{X}_{2} = \overrightarrow{X}_{\beta} - \overrightarrow{A}_{2}, (\overrightarrow{D}_{\beta}).\overrightarrow{X}_{3} = \overrightarrow{X}_{\delta} - \overrightarrow{A}_{3}, (\overrightarrow{D}_{\delta})$$

$$\overrightarrow{X}(t+1) = \frac{\overrightarrow{X}_{1} + \overrightarrow{X}_{2} + \overrightarrow{X}_{3}}{3}$$

$$(25)$$

In the modified Gray Wolf Optimization (GWO) algorithm, classification is performed based on a majority vote among neighboring solutions, determined using a distance function. The distance between points is calculated using Equation (26).

$$d = \sqrt{\sum_{i=1}^{k} (x_i - y_i)^2}$$
 (26)

where k is the number of points.

In this modified approach, the following equation is used in place of Equation (25) to generate the positions for the next iteration.

$$\vec{X}(t+1) = \frac{\overrightarrow{X_1} + \overrightarrow{X_2} + \overrightarrow{X_3} + \overrightarrow{X_{KNN}}}{4} \tag{27}$$

The above relationship results in better performance of the algorithm for searching for the overall optimal solution[9].

#### 4. FORMULATION OF THE PERFORMANCE-BASED DESIGN PROBLEM FOR STEEL SHEAR WALL SYSTEMS

The performance-based optimization problem can be formulated as follows:

minimize: 
$$F(x)$$
 (28)

subject to: 
$$g_i^S(x) \le 0 \quad i = 1 \cdot 2 \cdot \dots \cdot n$$
 (29) 
$$g_i^{PBD}(x) \le 0 \quad i = 1 \cdot 2 \cdot \dots \cdot n$$
 (30)

$$g_i^{PBD}(x) \le 0 \cdot i = 1.2 \cdot \dots \cdot n \tag{30}$$

In the above expressions,  $g_i^s$  represents the member stress constraints under gravity loads, applied in accordance with ANSI/AISC 341-22 [23], while  $g_i^{PBD}$  denotes the constraints related to performance-based design, which are defined as follows:

The allowable inter-story drift limits for various performance levels are determined using the following formula:

$$g_1 = \frac{\Delta^i}{(\Delta^i)_{all}} - 1 \le 0 \qquad i = IO \cdot LS \cdot CP \tag{31}$$

where  $\Delta$  is the inter-story drift, and  $(\Delta)_{all}$  is the allowable inter-story drift for each performance level as specified in FEMA-356, presented in Table 1 [12,13].

Table 1: Permissible values of floor drift

Performance level	$(\Delta)_{all}$
IO	0.5%
LS	2.5%
СР	5%

The possible failure mechanisms in beams, according to FEMA-356, are deformationcontrolled (DC) actions at various performance levels. The acceptance criteria are determined based on the plastic rotation capacity of the beams, as expressed in Formula 32.

$$g_2 = \frac{\theta^i}{(n\theta_y)} - 1 \le 0 \qquad i = IO \cdot LS \cdot CP \tag{32}$$

where  $\theta$  is the plastic rotation of the beam at each performance level, n is a coefficient determined from Table 5-6 of FEMA-356 based on the compactness classification of the steel sections, and  $\theta_{\nu}$  is the yield rotation calculated using Eq. 33.

$$\theta_y = \frac{ZF_{ye}l_b}{6FI_b} \tag{33}$$

where Z is the plastic section modulus,  $F_{ye}$  is the expected yield stress of the steel,  $l_b$  is the member length, and E is the modulus of elasticity.

The acceptance criteria for columns in performance-based design are defined based on controlling the possible failure mechanisms within the column. To accomplish this, force-controlled (FC) and deformation-controlled (DC) actions must be identified at various performance levels. Columns subjected to bending moments, in which the axial force at the target displacement is less than 50% of the lower limit compressive strength  $P_{CL}$ , are classified as deformation-controlled (DC). In such cases, the maximum allowable plastic rotation for each column is defined as follows:

$$g_{DC.i}^{p/50}(X) = \frac{\theta_i^{p/50}}{\theta_{p.i}^{p/50}} - 1 \le 0 \cdot i = 1.2....nc$$
 (34)

where  $\theta_i^{p/50}$  is the maximum plastic rotation of the *i*th column at the risk level p/50, and  $\theta_{p,i}^{p/50}$  is the allowable plastic rotation of the *i*th column, defined according to Table 5-6 of FEMA 356, based on the axial force and seismic compression conditions of the steel section. Here, nc represents the total number of columns.

Columns subjected to combined bending and shear forces at a target displacement greater than or equal to 50% of the column's lower limit compressive strength  $P_{CL}$  are classified as force-controlled. For these columns, the maximum plastic rotation constraint is defined as follows:

$$g_{FC.i}^{p/50}(X) = \frac{P_{UF.i}^{p/50}}{P_{CL}} + \frac{M_{UF.i}^{p/50}}{M_{CL}} - 1 \le 0 \cdot i = 1.2....nc$$
 (35)

where  $P_{UF,i}^{p/50}$  and  $M_{UF,i}^{p/50}$  represent the axial and moment forces, respectively, acting on the *i*th column due to gravity loads combined with seismic forces under force-controlled conditions at the hazard level p/50.  $P_{CL}$  and  $M_{CL}$  denote the lower limit compressive strength and flexural strength of the column, respectively.

The acceptance criteria for steel shear walls, based on FEMA-356 and ASCE/SEI 41-17, are presented in Table 2.

Table 2: Acceptance criteria for steel shear walls according to FEMA-356

	IO	LS	CP
Plastic Rotation Angle, Radians	$0.5\theta_y$	$10\theta_y$	$13\theta_y$

The maximum plastic rotation constraint for each steel shear wall is defined as follows:

$$g_{PD.i}^{p/50}(X) = \frac{\theta_{i.w}^{p/50}}{\theta_{pw.i}^{p/50}} - 1 \le 0 \quad i = 1.2 \dots nw$$
 (36)

where  $\theta_{i.w}^{p/50}$  is the maximum plastic rotation of the *i*th shear wall at the risk level p/50,  $\theta_{pw.i}^{p/50}$  is the allowable rotation of the ith shear wall as defined in Table 2, and nw is the number of steel shear walls.

To calculate  $\theta_y$ , the following formula can be used [24,25]:

$$\theta_{y} \approx \frac{\delta_{y}}{H}$$
 (37)

where  $\delta_y$  is the lateral displacement at yield (corresponding to the first yield of the steel plate), and H is the height of the story. To calculate  $\delta_y$ , the yield shear strength of steel shear walls can be determined using the tensile field theory, which accounts for the buckling behavior of thin plates, as follows:

$$\delta_y = \frac{V_y}{K} \tag{38}$$

where  $V_y$  is the yield shear strength and K is the initial lateral stiffness of the steel shear wall system at the desired story.

According to FEMA-356 and ANSI/AISC 341-22, the yield shear strength  $V_y$  of a steel shear wall can be calculated using the following formula:

$$V_v = 0.42 f_v t_w L_{cf} \sin 2\alpha \tag{39}$$

where  $f_y$  is the yield stress of the steel shear wall plate,  $t_w$  is the thickness of the steel shear wall plate,  $L_{cf}$  is the net length of the steel shear wall, and  $\alpha$  is the angle of inclination of the tension field.

The initial lateral stiffness of the steel shear wall system K can be obtained by initial elastic analysis of the system.

Another important aspect in the design of steel frames is the consideration of implementation-related constraints, such as beam-to-column and column-to-column connection constraints, which are incorporated in this study. The open-source software OpenSees is utilized for finite element modeling of the structures, while MATLAB is employed to implement the optimization algorithms and perform the necessary calculations.

#### 5. SEISMIC COLLAPSE SAFETY ASSESSMENT

Ensuring the seismic safety of structural systems, particularly under extreme ground motions, is a central objective in performance-based earthquake engineering. While traditional design methods target life safety at specific hazard levels, collapse safety under Maximum Considered Earthquake (MCE) conditions is a critical performance objective for essential and high-rise buildings. To address this, the FEMA-P695 [26] methodology provides a rigorous framework to evaluate the collapse safety of structural systems through nonlinear dynamic analysis, particularly suitable for innovative or optimized structural solutions.

The assessment begins with Incremental Dynamic Analysis (IDA) of each archetype. Each structural model is subjected to a suite of 22 far-field ground motion records (Table 3), incrementally scaled in terms of their spectral acceleration at the structure's first-mode period T1. For each record, the onset of collapse is identified as the point of dynamic instability or numerical divergence in the nonlinear analysis. The corresponding collapse spectral acceleration values  $Sa_{collapse}$  for each ground motion are recorded. From the set of 22 collapse intensities, the median spectral acceleration at collapse,  $S_{CT}$ , is calculated:

$$S_{CT} = median(Sa_{collapse,1}, Sa_{collapse,2}, ..., Sa_{collapse,22})$$
(40)

The Collapse Margin Ratio (*CMR*) is then computed by comparing the median collapse capacity  $S_{CT}$  to the MCE-level demand  $S_{MCE}(T_1)$ , derived from the design spectrum:

$$CMR = \frac{S_{CT}}{S_{MCE}(T_1)} \tag{41}$$

while the *CMR* provides an initial measure of collapse capacity, it does not account for modeling uncertainties and ground motion variability. Thus, FEMA P-695 introduces the Adjusted Collapse Margin Ratio (*ACMR*):

$$ACMR = CMR \times SF(\beta_{TOT}) \tag{42}$$

Where  $SF(\beta_{TOT})$  is a safety factor determined from FEMA P-695 Table 7-2 and depends on the total system uncertainty  $\beta_{TOT}$ , calculated as:

$$\beta_{TOT} = \sqrt{\beta_{RTR}^2 + \beta_{MDL}^2 + \beta_{QNT}^2} \tag{43}$$

 $\beta_{RTR}$  (Record-to-Record Variability): Set to 0.55 as a FEMA-recommended default, unless project-specific values are used.

 $\beta_{MDL}$  (Modeling Uncertainty): For the 10- and 15-story SPSW frames modeled in OpenSees using validated nonlinear fiber sections and plate shear wall components, a value of 0.25 is adopted.

 $\beta_{QNT}$  (Quality of System Knowledge): Set to 0.0 for well-established systems like steel SPSW.

For archetypes of this study:

$$\beta_{TOT} = \sqrt{0.55^2 + 0.25^2 + 0^2} = 0.6$$

with  $\beta_{TOT}$ =0.60, the corresponding safety factor  $SF(\beta_{TOT})$  from FEMA P-695 is approximately 0.78, and the  $ACMR_{target}$ , is 1.96.

The final collapse safety check is performed by comparing the computed ACMR to the target value:

This condition must be met to confirm that the structure has a low enough probability of collapse ( $\leq 10\%$ ) under MCE-level shaking, as required by FEMA P-695.

By applying this methodology to optimized archetypes, this study not only assesses their seismic collapse safety but also validates the robustness of the applied optimization strategy. The results provide essential evidence on the effectiveness of performance-based optimization when verified under collapse-level earthquake demands.

Table 3: Ground motion records set

Name	M	Year	Record Station
		1994	
Northridge	6.7		Beverly Hills - Mulhol
Northridge	6.7	1994	Canyon Country-WLC
Duzce, Turkey	7.1	1999	Bolu
Hector Mine	7.1	1999	Hector
Imperial Valley	6.5	1979	Delta
Imperial Valley	6.5	1979	El Centro Array #11
Kobe, Japan	6.9	1995	Nishi-Akashi
Kobe, Japan	6.9	1995	Shin-Osaka
Kocaeli, Turkey	7.5	1999	Duzce
Kocaeli, Turkey	7.5	1999	Arcelik
Landers	7.3	1992	Yermo Fire Station
Landers	7.3	1992	Coolwater
Loma Prieta	6.9	1989	Capitola
Loma Prieta	6.9	1989	Gilroy Array #3
Manjil, Iran	7.4	1990	Abbar
Superstition Hills	6.5	1987	El Centro Imp. Co.
Superstition Hills	6.5	1987	Poe Road (temp)
Cape Mendocino	7.0	1992	Rio Dell Overpass
Chi-Chi, Taiwan	7.6	1999	CHY101
Chi-Chi, Taiwan	7.6	1999	TCU045
San Fernando	6.6	1971	LA - Hollywood Stor
Friuli, Italy	6.5	1976	Tolmezzo

#### 6. NUMERICAL EXAMPLES

In this study, the optimal vertical placement of steel shear walls within the structure is determined using performance-based design principles and various metaheuristic optimization algorithms. Due to the potential for irregularities in the lateral load-resisting system—particularly Out-of-Plane Offset Irregularity—linear static analyses are not permitted in the optimization process of steel frames with steel shear wall systems, in accordance with the provisions of ASCE/SEI 7-22 [27] and FEMA-356. These regulations mandate the use of nonlinear analysis methods for such structural configurations to accurately capture their seismic behavior and ensure code compliance.

The analysis used in the optimization process is a nonlinear static pushover analysis, and performance-based design principles are employed to evaluate and control the structural performance. The structures examined in this study consist of 5-span frames with 10 and 15 stories. Member grouping is carried out such that the exterior and interior columns are assigned to two distinct groups over every two consecutive stories. Similarly, the grouping of beams and steel shear walls follows a two-story grouping scheme, as illustrated in Figure 4. The cross-sections of beam and column members are selected from standard W-shaped sections, as well as the thickness of the shear wall plate, according to Table 4. The applied dead and live loads on the beams are 24.5 kN/m and 25.5 kN/m, respectively. All beam, column, and steel shear wall elements have a yield stress of 235 MPa with a post-yield hardening ratio of 3%. The unit weight of steel is taken as 76.82 kN/m³, and the modulus of elasticity is assumed to be 200 GPa. To preserve the symmetry of the frames, six distinct vertical configurations for steel shear wall placement are considered in optimizing the structural layout, as depicted in Figure 4.

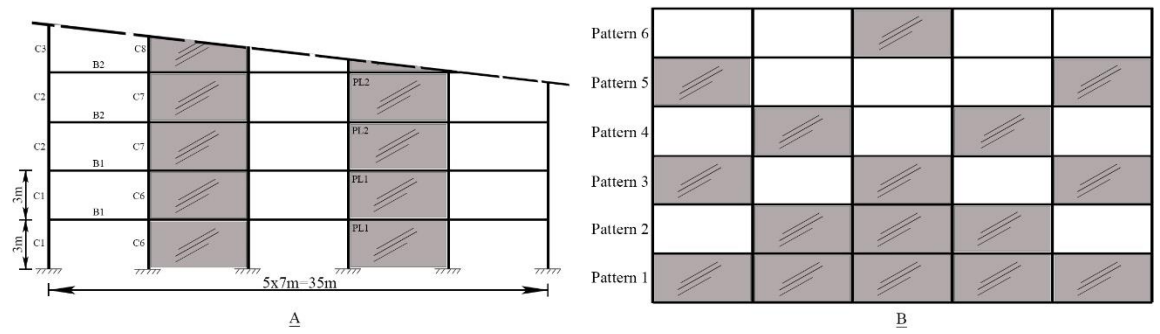


Figure 4: (A) Dimensions and grouping (B) Positioning patterns of steel shear walls

Beams and Columns						Thickn	ess of shear wall plates
No.	Profile	No.	Profile	No.	Profile	No.	Profile
1	W14×22	11	W14×74	21	W14×193	1	1 mm
2	W14×26	12	W14×82	22	W14×211	2	2 mm
3	W14×30	13	W14×90	23	W14×233	3	3 mm
4	W14×34	14	W14×99	24	W14×257	4	4 mm
5	W14×38	15	W14×109	25	W14×283	5	5 mm
6	W14×43	16	W14×120	26	W14×311	6	6 mm
7	W14×48	17	W14×132	27	W14×342	7	7 mm
8	W14×53	18	W14×145	28	W14×370	8	8 mm
9	W14×61	19	W14×159	29	W14×398	9	9 mm
10	W14×68	20	W14×176	30	W14×426	10	10 mm

Table 4: The available list of standard sections

In this study, the seismic collapse performance of 10- and 15-story steel frames with steel plate shear wall (SPSW) systems is assessed. These frames have been previously optimized using performance-based design (PBD) methods to achieve efficient structural layouts and optimal member sizing. The current objective is to validate these optimized designs by assessing their seismic collapse performance using the FEMA P-695 procedure.

#### 6.1 Example 1: 10-story SPSW

To optimize a 10-story steel frame equipped with a steel shear wall lateral restraint system, the Modified Dolphin echolocation Algorithm (MDE) was configured with a population size of 40 structures per iteration and run for 400 iterations. The Center of mass optimization algorithm (CMO) was set with 400 iterations and 40 structures per iteration. The Modified Gray Wolf (KNN) algorithm was executed with 400 iterations and a population of 40 structures per iteration. Initially, the optimization was conducted assuming fixed, common positions for the steel shear walls located at spans 2 and 4 as well as spans 1 and 5 along the building height. Subsequently, the positions of the shear walls were incorporated as design variables to allow their optimization. To enhance the robustness of the results and reduce the risk of convergence to local optima, each optimization algorithm was independently run 10 times using the specified iteration counts. Table 5 summarizes the structural section selections according to Table 4 and the corresponding weights obtained from each algorithm. It is evident from the results that the best statistical performance was achieved by the Modified Dolphin echolocation Algorithm (MDE).

Table 5: PBD topology optimization results for 10-story SPSW

Grouping		KNN			CMO			MDE	
	Fixed position Optimal Fixed position Optimal	Fixed p	osition	Optimal					
	spans 1&5	spans 2&4	position	spans 1&5	spans 2&4	position	spans 1&5	spans 2&4	position
C1	19	20	19	20	20	19	20	20	18
C2	18	19	18	18	18	17	19	18	16
C3	17	17	16	16	18	17	17	17	13
C4	14	15	14	14	16	13	16	15	11
C5	12	11	11	11	12	11	13	12	10
C6	19	19	18	19	18	17	19	18	17
C7	18	17	16	17	17	16	17	17	15
C8	16	15	15	15	15	15	16	15	15
С9	15	15	15	13	14	15	14	14	14
C10	11	10	10	11	11	10	11	12	10
B1	10	10	10	11	10	9	10	11	10
B2	11	10	9	10	10	10	10	10	9
В3	9	10	9	9	10	9	9	9	9
B4	9	9	8	9	9	8	8	9	8
B5	8	8	8	8	8	8	8	8	7
PL1(mm)	5.00	5.00	4.00	5.00	5.00	4.00	5.00	5.00	5.0
PL2(mm)	4.00	4.00	4.00	5.00	4.00	5.00	5.00	4.00	5.00
PL3(mm)	4.00	4.00	4.00	4.00	4.00	4.00	4.00	4.00	4.00
PL4(mm)	3.00	3.00	4.00	4.00	3.00	3.00	3.00	3.00	4.00
PL5(mm)	2.00	2.00	2.00	2.00	2.00	2.00	2.00	2.00	2.00
Weight(kg)	77621	77175	74736	77332	76863	73404	77050	76637	69485
Deviation from the standard	943	984	1184	924	907	1105	893	865	1023
Percentage of best result	9.25%	8.62%	5.19%	8.84%	8.18%	3.32%	8.45%	7.87%	

Figure 5 illustrates the optimal locations of the steel shear walls as determined by the optimization algorithms. Figure 6 presents the convergence curves of the (MDE) algorithm for the 10-story frame, comparing results for fixed shear wall positions at spans 1 and 4 with those obtained from the optimized shear wall placements.

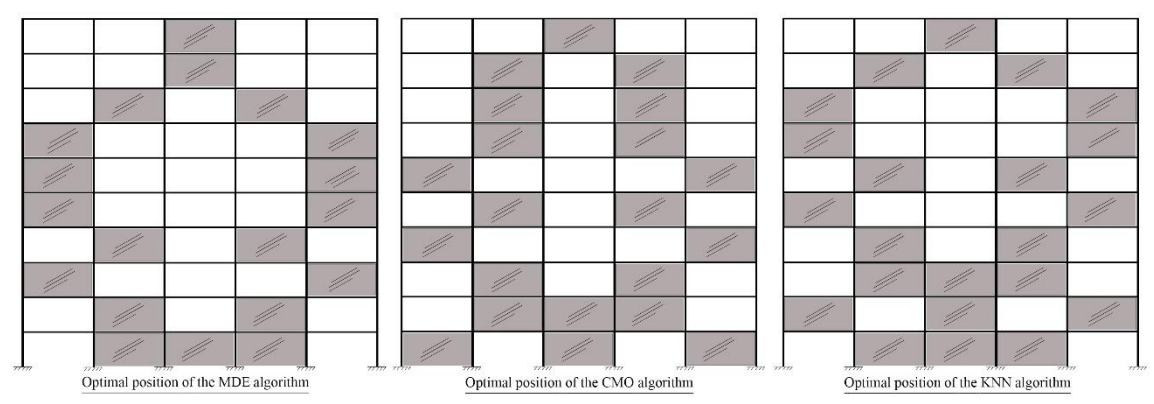


Figure 5: optimal positions obtained by algorithms for a 10-story SPSW

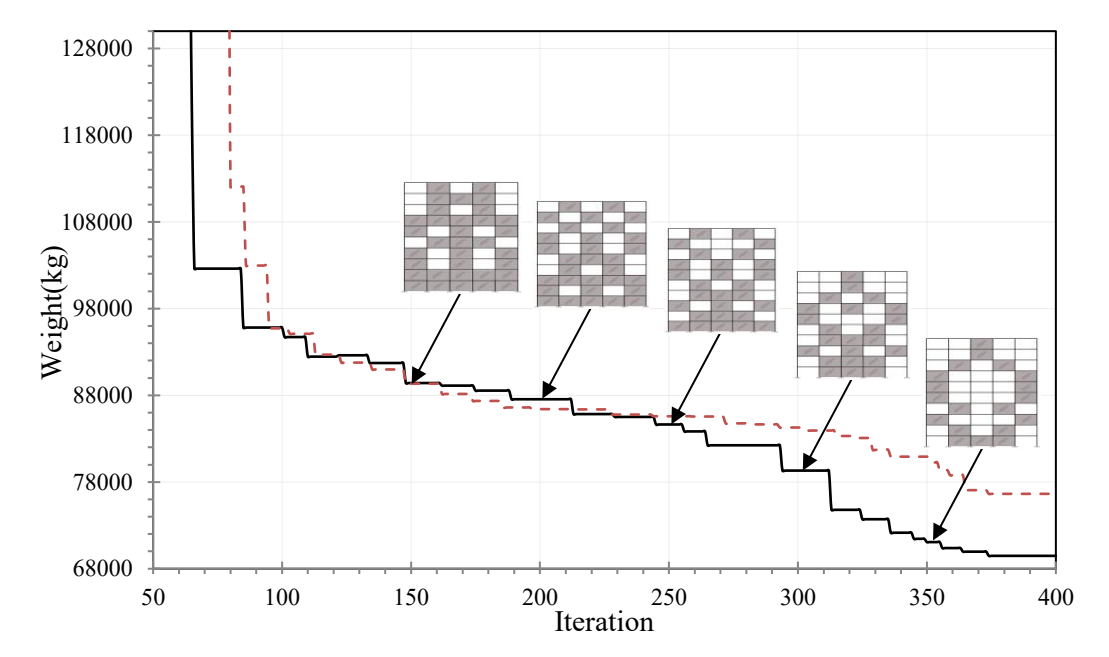


Figure 6: Convergence curves of MDE algorithms for fixed position in spans 2 and 4 and placement of shear walls of 10-story structure

Figure 7 shows the pushover diagram of the most optimal 10-story frames with fixed position and optimal placement of steel shear walls under the lateral load pattern according to  $C_{vx}$  (Formula 2).

The design process constraints for the 10-story frame include the story drift limit at the Immediate Occupancy (IO) level, the plastic rotation limit of steel shear walls at the IO level, the force-controlled constraint  $g_{FC.i}^{2/50}$  for columns at the Collapse Prevention (CP) performance level, and the plastic rotation limits for both beams and columns at the CP level. Figure 8 illustrates the values of these constraints for the most optimal frames with fixed steel shear wall positions at spans 2 and 4, as well as for the frames with optimally placed steel shear walls. It is evident that all performance-based design constraints remain

within their allowable limits. The Incremental Dynamic Analysis (IDA) curves for the 10-story frame with the optimized configuration of steel plate shear walls are presented in Figure 9. The corresponding results of the seismic collapse safety assessment, based on FEMA P-695 methodology, are summarized in Table 6. As shown, the Adjusted Collapse Margin Ratio (ACMR) of the optimized frame exceeds the required target ACMR, indicating that the structure satisfies the collapse safety performance criteria and possesses sufficient seismic robustness.

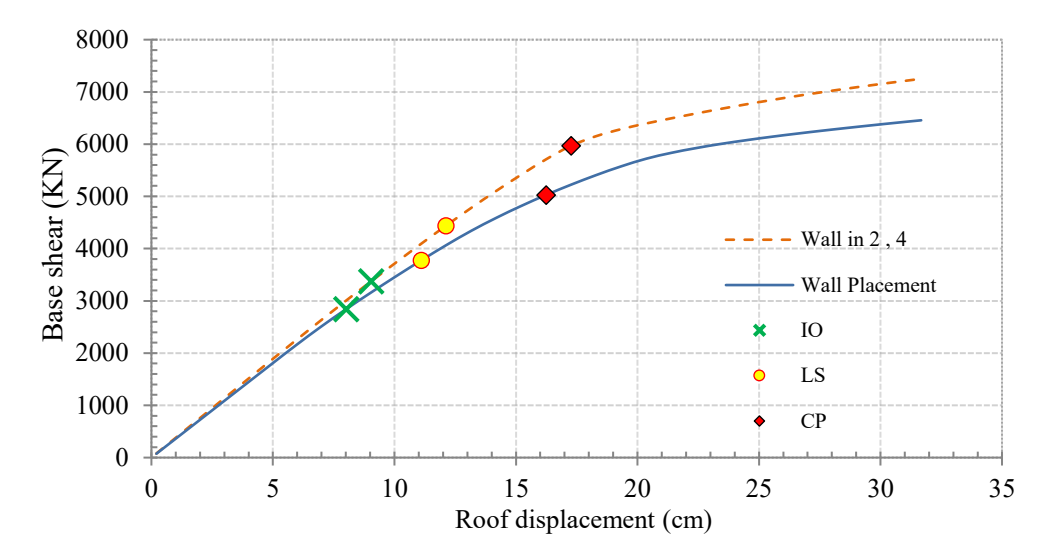


Figure 7: Pushover diagram under lateral load pattern  $C_{vx}$  for a 10-story structure

Table 6. Seismic collapse safety parameters for optimal 10-story

<b>Optimal Design</b>	CMR	SSF	ACMR	ACMR <sub>target</sub>	Pass/Fail
10Story	2.92	0.78	2.28	1.96	P

#### 6.2 Example 2: 15-story SPSW

To optimize a 15-story steel frame equipped with a steel shear wall lateral restraint system, the Modified Dolphin echolocation Algorithm (MDE) was configured with a population size of 40 structures per iteration and run for 500 iterations. The Center of mass optimization algorithm (CMO) was set with 500 iterations and 40 structures per iteration. The Modified Gray Wolf (KNN) algorithm was executed with 500 iterations and a population of 40 structures per iteration. Initially, the optimization was conducted assuming fixed, common positions for the steel shear walls located at spans 2 and 4 as well as spans 1 and 5 along the building height. Subsequently, the position of the shear walls is treated as a design variable. To ensure the attainment of a global optimum and prevent convergence to local optima, the optimization process is repeated 10 times for each algorithm with the specified iteration counts. Table 7 presents the structural sections based on Table 4 along with the weights obtained from each algorithm. It is observed that the best result for the optimal placement of steel shear walls is achieved by the MDE algorithm, while the best

result for fixed-position steel shear walls corresponds to the CMO algorithm with walls located at spans 2 and 4. Figure 10 illustrates the optimal wall positions obtained by the optimization algorithms. Additionally, Figure 11 displays the convergence curves of the best results for the 15-story frame with fixed steel shear wall positions at spans 1 and 4 (by the CMO algorithm) as well as the optimal shear wall placements determined by the MDE algorithm.

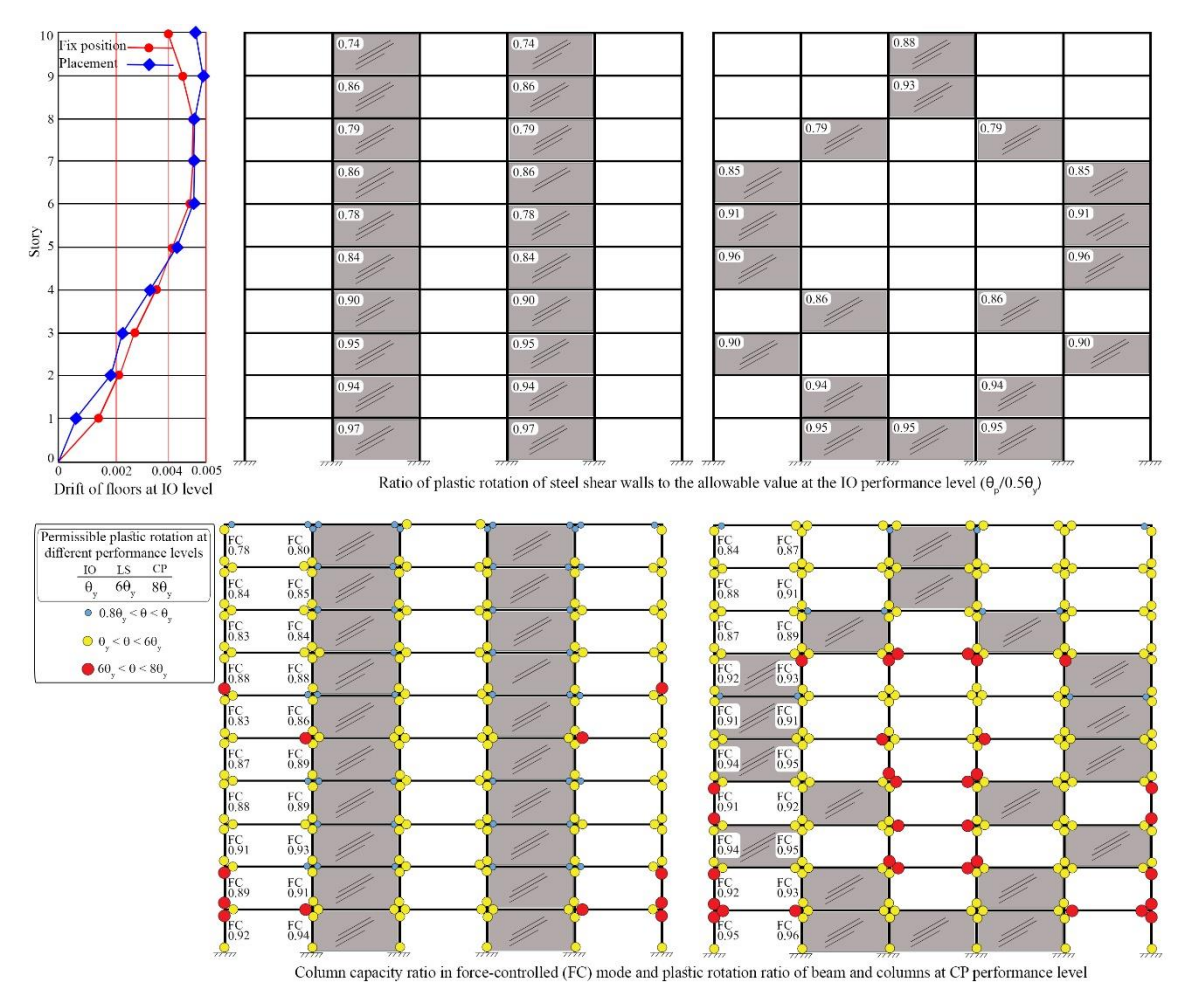


Figure 8: Active design constraints for optimal 10-story frames

Figure 12 shows the pushover diagram of the most optimal 15-story frames with fixed position and optimal placement of steel shear walls under the lateral load pattern according to  $C_{vx}$  (Formula 2).

The design of the 15-story frame is governed by code constraints including the story drift limit at the Immediate Occupancy (IO) level, the plastic rotation limit of steel shear walls at the IO level, the force-controlled constraint on columns expressed as  $g_{FC.i}^{2/50}$  at the Collapse Prevention (CP) performance level, and the plastic rotation constraints for beams and columns at the CP level. Figure 13 presents the values of these constraints for the most optimal frames with steel shear walls fixed at spans 2 and 4, as well as for frames with

optimally placed shear walls. It is evident that all performance-based design constraints remain within their allowable limits.

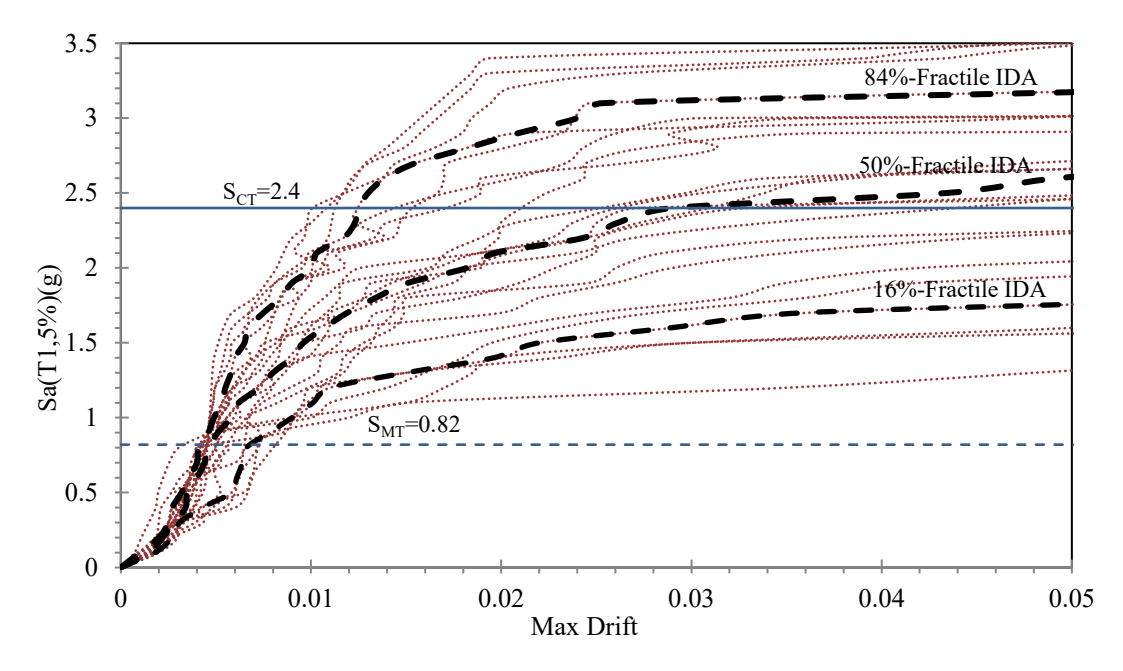


Figure 9: IDA curves for the 10-story frame with the optimized configuration of steel plate shear walls

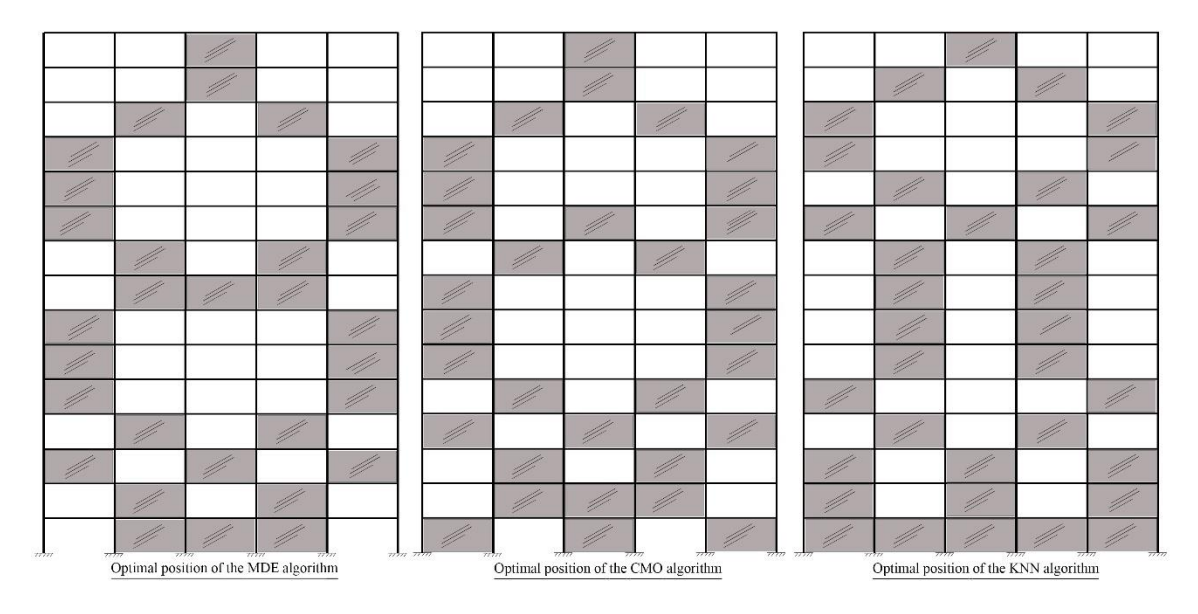


Figure 10: optimal positions obtained by algorithms for a 15-story SPSW

The Incremental Dynamic Analysis (IDA) curves for the 15-story frame with the optimized configuration of steel plate shear walls are presented in Figure 14. The

corresponding results of the seismic collapse safety assessment, based on FEMA P-695 methodology, are summarized in Table 8. As shown, the Adjusted Collapse Margin Ratio (ACMR) of the optimized frame exceeds the required target ACMR, indicating that the structure satisfies the collapse safety performance criteria and possesses sufficient seismic robustness.

Table 7: PBD topology optimization results for 15-story SPSW

Grouping		KNN			CMO			MDE	
<del>-</del>	Fixed p		Optimal position			Optimal position	Fixed p	osition	Optimal position
	spans 1&5	spans 2&4	1	spans 1&5	spans 2&4	r	spans 1&5	spans 2&4	- 1
C1	23	25	22	23	25	23	23	24	22
C2	22	23	20	22	23	21	22	22	21
C3	20	22	19	21	21	19	20	19	18
C4	20	20	18	19	19	17	19	18	16
C5	19	18	17	18	17	16	17	16	15
C6	15	14	14	16	15	15	15	15	15
C7	12	12	13	13	12	12	14	13	12
C8	10	10	11	10	10	11	11	10	11
C9	23	24	21	22	23	22	23	23	21
C10	22	21	19	21	21	20	22	22	19
C11	20	20	19	21	19	19	20	19	19
C12	19	18	18	19	17	19	19	19	18
C13	19	15	17	18	16	16	19	16	16
C14	16	15	16	17	14	16	16	14	15
C15	13	13	12	14	13	11	14	13	11
C16	11	10	11	10	10	10	11	10	10
B1	10	10	9	10	9	9	10	10	9
B2	9	9	10	9	9	9	10	9	9
В3	10	9	9	10	10	10	9	10	9
B4	9	8	9	10	8	9	9	9	8
B5	9	8	8	9	8	8	10	8	8
В6	9	8	9	9	9	9	9	9	9
В7	8	8	8	8	8	8	8	8	7
B8	8	7	7	8	7	7	8	7	7
PL1(mm)	6.00	6.00	5.00	6.00	6.00	5.00	6.00	6.00	6.00
PL2(mm)	5.00	6.00	5.00	5.00	6.00	5.00	5.00	6.00	5.00
PL3(mm)	5.00	5.00	5.00	5.00	5.00	5.00	5.00	5.00	5.00
PL4(mm)	4.00	5.00	5.00	4.00	5.00	4.00	4.00	5.00	4.00
PL5(mm)	4.00	4.00	3.00	4.00	4.00	4.00	4.00	4.00	4.00
PL6(mm)	3.00	4.00	4.00	3.00	4.00	4.00	3.00	3.00	4.00
PL7(mm)	3.00	3.00	3.00	3.00	3.00	3.00	2.00	3.00	3.00
PL8(mm)	2.00	2.00	2.00	2.00	2.00	2.00	2.00	2.00	2.00
Weight(kg)	137145	134153	130786	137101	132437	129935	137113	133174	124689
Deviation from the standard	1387	1342	1694	1308	1193	1624	1286	1204	1541
Percentage of best result	9.98%	7.59%	4.88%	9.95%	6.21%	4.21%	9.96%	6.80%	

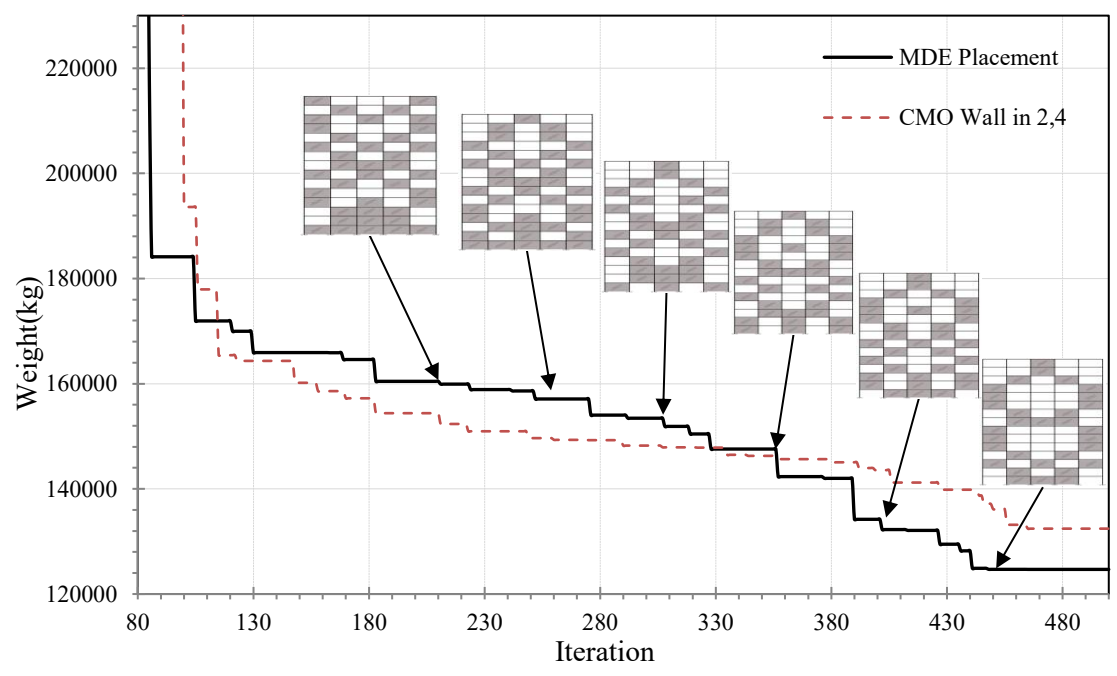


Figure 11: Convergence curves of MDE algorithms for fixed position in spans 2 and 4 and placement of shear walls of 15-story structure

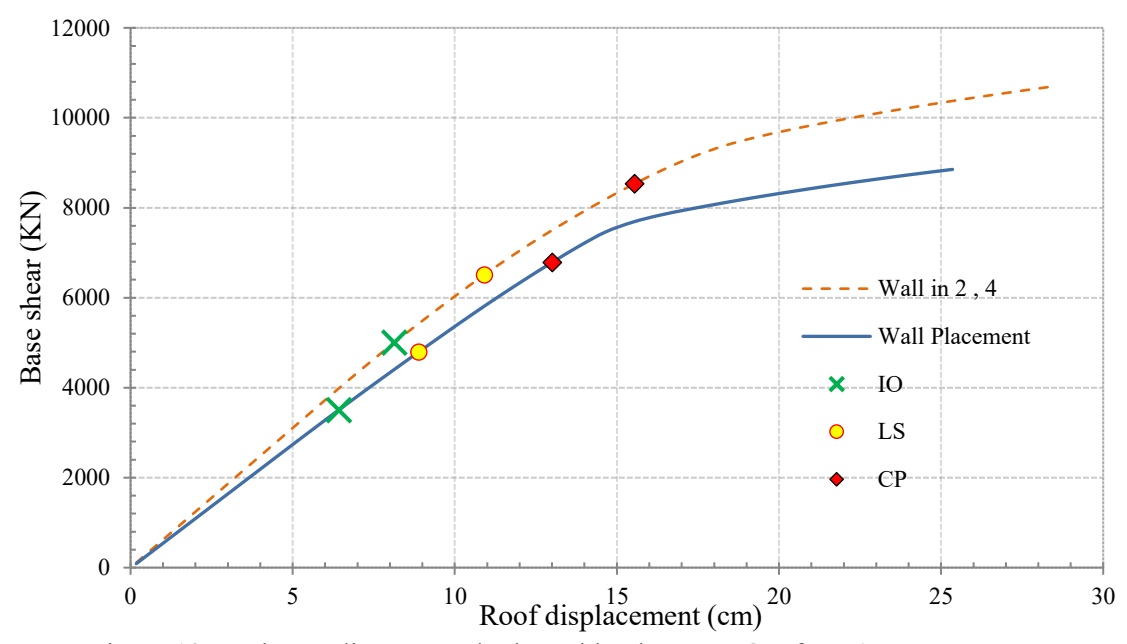


Figure 12: Pushover diagram under lateral load pattern  $\boldsymbol{C}_{\boldsymbol{v}\boldsymbol{x}}$  for a 15-story structure

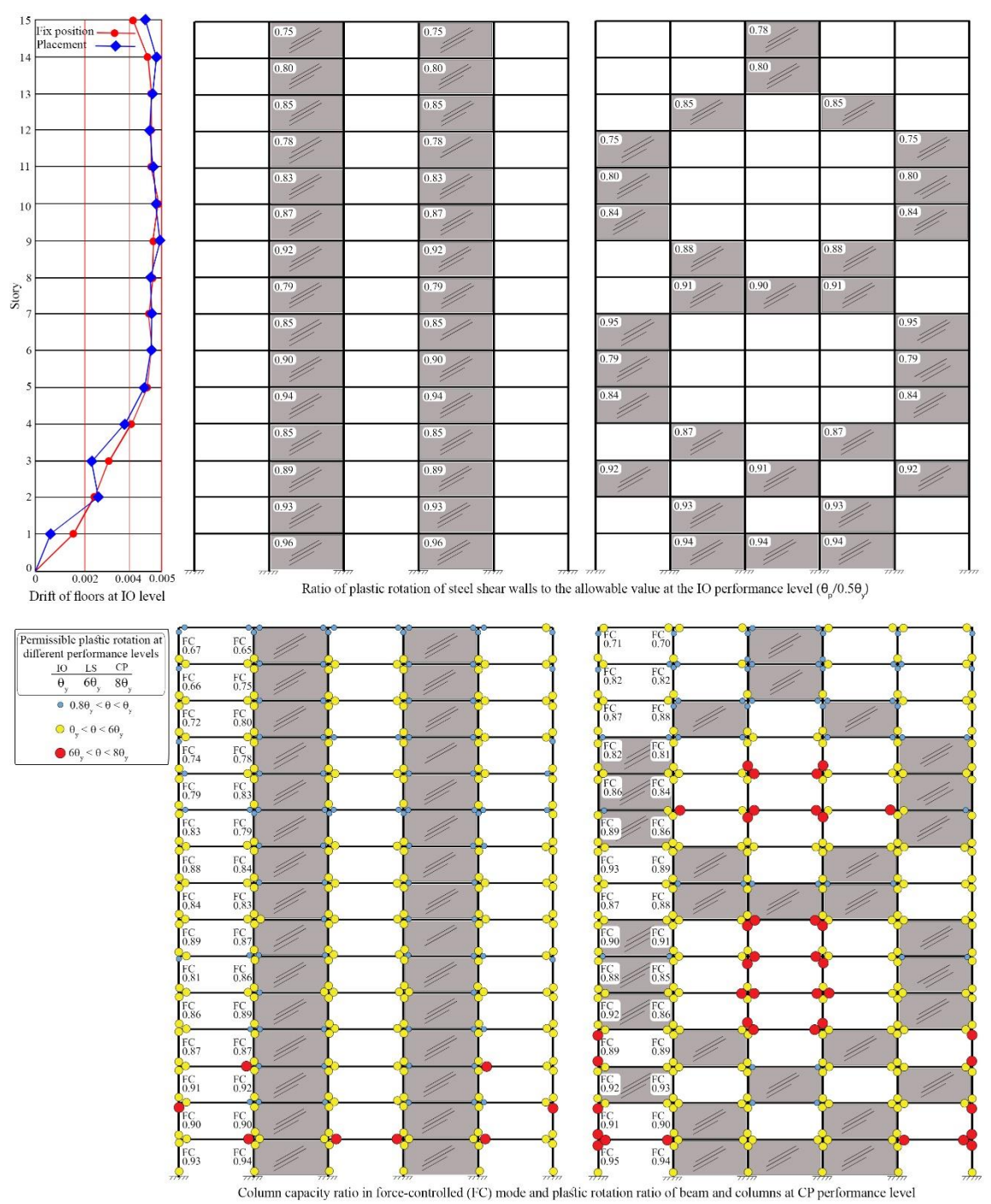


Figure 13: Active design constraints for optimal 15-story frames

Table 8: Seismic collapse safety parameters for optimal 15-story

<b>Optimal Design</b>	CMR	SSF	ACMR	ACMR <sub>target</sub>	Pass/Fail
15Story	3.75	0.78	2.92	1.96	P

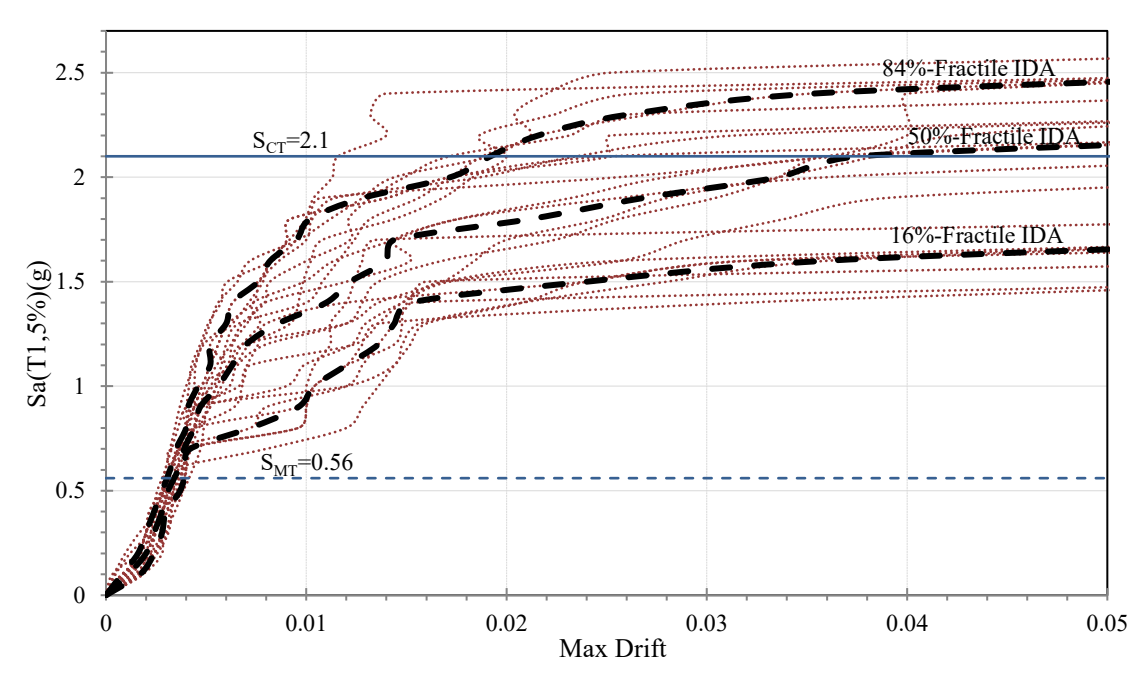


Figure 14: IDA curves for the 15-story frame with the optimized configuration of steel plate shear walls

#### 7. CONCLUSIONS

In this study, 10- and 15-story frames with a steel shear wall lateral load-bearing system were optimized using three different metaheuristic algorithms. Initially, the structures were optimized considering fixed, conventional wall positions along the height; subsequently, the positions of the shear walls were treated as design variables. The selection of algorithms was based on their demonstrated performance in addressing similar problems reported in the literature.

A key finding from the optimization process is the significant influence of shear wall location on the optimal structural weight. For instance, using the MDE algorithm, the optimal placement of walls contributed to approximately a 7 to 8 percent reduction in structural weight. Regarding algorithm performance, for the 10-story structure, the MDE algorithm outperformed others, achieving an optimal weight that is 3.32% and 5.19% lower than those obtained by the CMO and KNN algorithms, respectively. Furthermore, for the fixed wall position scenario, the MDE algorithm also provided the lowest optimal weight among all algorithms tested.

For the 15-story structure, the MDE algorithm similarly exhibited superior performance in optimizing wall placement, delivering an optimal weight reduction of 4.21% compared to the CMO algorithm and 4.88% compared to the KNN algorithm. However, when wall positions were fixed, the CMO algorithm yielded the lightest design among the methods considered.

Analysis of active design constraints in the performance-based design of both 10- and 15-

story frames revealed that optimal shear wall placement significantly enhances the utilization of the structure's strength and ductility capacities. The optimal configuration tends to locate shear walls in regions of high demand, leading to the simultaneous activation of multiple design constraints during the optimization process. This highlights the notable efficacy of metaheuristic algorithms in addressing complex nonlinear optimization problems by minimizing structural weight while ensuring all governing constraints approach their allowable limits, thereby producing highly efficient designs relative to the objective function.

To evaluate the seismic performance of the proposed structural design, Incremental Dynamic Analysis (IDA) was performed on both the shape-optimized 10- and 15-story frames. The results of these nonlinear dynamic analyses were used to assess the seismic collapse capacity of the structures in accordance with FEMA P-695 guidelines. The obtained results showed that the optimized designs meet the acceptable seismic safety requirements defined by FEMA P-695 and confirmed their reliability under severe seismic demands. Additionally, the results emphasize the importance of accounting for out-of-plane offset irregularities in the lateral load-bearing system when determining the optimal shear wall layout. The application of nonlinear static and dynamic analyses, combined with performance-based design methodologies, effectively captures the increased stresses and deformations associated with such irregularities. Consequently, conventional linear analyses and force-based design approaches are insufficient for accurately predicting the performance and capacity of structures exhibiting these discontinuities, underscoring the necessity for advanced nonlinear methods in seismic design and optimization.

#### REFERENCES

- 1. A.Kaveh, A.Nasrollahi, Performance-based seismic design of steel frames utilizing charged system search optimization, Applied Soft Computing 2014; 22: 213-21.
- 2. A.Kaveh, K. Laknejadi, B. Alinejad, Performance-based multi-objective optimization of large steel structures, *Acta Mech* 2012; **232**: 355–69.
- 3. S.Gholizadeh, M.Ebadijalal, Performance based discrete topology optimization of steel braced frames by a new metaheuristic, Advances in Engineering Software 2018; 123: 77–92
- 4. Nikos D. Lagaros, Anargyri Th. Garavelas, Manolis Papadrakakis, Innovative seismic design optimization with reliability constraints, Comput. Methods Appl. Mech. Engrg 2008; **198**: 28–41.
- 5. Peng Pan, Makoto Ohsaki, Takuya Kinoshita, Constraint approach to performance-based design of steel moment-resisting frames, Engineering Structures 2007; **29**: 186–94.
- 6. Astaneh-Asl A, Steel tips: seismic behaviour and design of steel shear walls. Technical report. Moraga (CA, USA):Structural Steel Educational Council 2001.
- 7. Ghosh.S, Adam.F, Das.A, Design of steel plate shear walls considering inelastic drift demand. Journal of Constructional Steel Research 2009; **65**: 1431–37.
- 8. Amir Saedi Daryan, Mohadeseh Salari, Soheil Palizi, Neda Farhoudi, Size and layout optimum design of frames with steel plate shear walls by metaheuristic optimization algorithms, Structures 2023; **48**: 657–68.

- 9. Reema Aswani1, S. P. Ghrera, Satish Chandra, A Novel Approach to Outlier Detection using Modified Grey Wolf Optimization and k-Nearest Neighbors Algorithm, Indian Journal of Science and Technology 2016; 44: 74-85.
- 10. Ganzerli.S, C.P.Pantelides, L.D.Reaveley, Performance-based design using structural optimization, Earthquake Engineering & Structural Dynamics, 2000; **29(11):** 1677-90.
- 11. Vamvatsicos D, Cornell CA, Incremental dynamic analysis, Earthquake Engineering and Structural Dynamics 2002; **31(3):** 491\_514.
- 12. FEMA-356, Prestandard and commentary for the seismic rehabilitation of buildings. Federal Emergency Management Agency, Washington, DC, 2000.
- 13. ASCE/SEI, Seismic Evaluation and Retrofit of Existing Buildings, American Society of Civil Engineers, 2017.
- 14. ANSI/AISC 360-22. Specification for structural steel buildings, American Institute of Steel Construction, August 1; 2022.
- 15. Kaveh A, Farahmand Azar B, Hadidi A, Rezazadeh Sorochi F, Talatahari S. Performance-based seismic design of steel frames using ant colony optimization. J Constr Steel Res 2010: **66:** 566–74.
- 16. Kunnath, S. K, Identification of modal combinations for nonlinear static analysis of building structures, Computer-Aided Civil and Infrastructure Engineering 2004; **19:** 282-95.
- 17. Berman.J, Seismic behavior of code designed steel plate shear walls, Engineering Structures 2011; **33:** 230 44.
- 18. Timler.P, Kulak.G, Experimental study of steel plate shear walls, Structural Engineering Report No. 114, Department of Civil and Environment Engineering, University of Alberta, Edmonton, Alberta, Canada 1983.
- 19. Driver.R, Kulak.G, Kennedy.D, Elwi.A, Seismic behavior of steel plate shear walls, Structural Engineering Report No. 215. Department of Civil and Environment Engineering, University of Alberta, Edmonton, Alberta, Canada 1997.
- 20. Berman.J, Bruneau.M, Experimental investigation of light-gauge steel plate shear walls, J. Struct. Eng, ASCE 2005; **131:** 259 67.
- 21. S.Mirjalili, S.Mirjalili, A.Lewis, Grey Wolf Optimizer, Advances in Engineering Software 2014; **69:** 46-61.
- 22. A.Kaveh, N. Farhoudi, A new optimization method: Dolphin echolocation, Advances in Engineering Software 2013; **59:** 53–70
- 23. ANSI/AISC 341-22, Seismic Provisions for Structural Steel Buildings, An American National Standard, September 26, 2022.
- 24. Jeffrey Berman, Michel Bruneau, Plastic Analysis and Design of Steel Plate Shear Walls, ASCE 0733-9445~2003;129:11-1448.
- 25. Seyed Mohammad Ali Abbaspoor Haghighat, Ali Alibazi, Reza Moradifard, Lotfi Guizani, Munzer Hassan, Seismic Evaluation of Steel Plate Shear Walls in Different Configurations, Journal of Rehabilitation in Civil Engineering 2025; 13: 81-109.
- 26. FEMA-P695. Quantification of building seismic performance factors. Washington (DC): Federal Emergency Management Agency, 2009.
- 27. ASCE/SEI 7-22, Minimum Design Loads and Associated Criteria for Buildings and Other Structures, American Society of Civil Engineers 2022.

- 28. M.Rezaei, Seismic Behaviour of Steel Plate Shear Walls By Shake Table Testing, B.A.SC.Iran university of science and technology,1990.
- 29. M.Kurata, R.T. Leon, R. DesRoches, M. Nakashima, Steel plate shear wall with tension-bracing for seismic rehabilitation of steel frames, Journal of Constructional Steel Research 2012; 71: 92 103.
- 30. Swapnil.B, Siddhartha Ghosh, Performance-based plastic design of steel plate shear walls, Journal of Constructional Steel Research 2013; **90:** 85–97.
- 31. Bing Qu, Xuhua Guo, Haoyan Chi, Michael Pollino, Probabilistic evaluation of effect of column stiffness on seismic performance of steel plate shear walls, Engineering Structures 2012; **43**: 169–79.
- 32. OpenSees version 2.4.4 [Computer software]. PEER, Berkeley, CA n.d.
- 33. MATLAB. The language of technical computing. Math Works Inc. 2024.